Pergamon

Int. Comm. Heat Mass Transfer, Vol. 23, No. 1, pp. 101–114, 1996

0735-1933/96 $12.00 + .00

0735-1933(95)00088-7

CONVECTIVE HEAT TRANSFER BETWEEN A MOVING CYLINDER AND FLOWING NON-NEWTONIAN FLUIDS

Tian-Yih Wang
Department of Mechanical Engineering
Mingchi Institute of Technology
Taishan, Taipei, Taiwan, R.O.C.

(Communicated by J.P. Hartnett and W.J. Minkowycz)

ABSTRACT

An analysis of steady laminar forced convection heat transfer from a moving or stationary slender cylinder to a quiescent or flowing non-Newtonian fluid has been presented. A relative velocity parameter, γ, is proposed to serve as a controlling index that properly indicates the relative importance of the velocity of the slender cylinder and the velocity of the free stream. The value of this parameter lies between 0 and 1. Furthermore, the coordinates and dependent variables are transformed to yield computationally efficient numerical solution that are valid over the entire range of relative velocity parameter from the limiting case of a non-Newtonian fluid free stream flowing over a stationary cylinder (γ = 0) to the other limiting case of a moving cylinder in a quiescent non-Newtonian fluid (γ = 1). The effects of the relative velocity parameter, the transverse curvature parameter, the power-law viscosity index and the generalized Prandtl number on the velocity profiles, the temperature distributions and the heat transfer group are clearly illustrated.

Introduction

For the past years, the problems of classical convective heat transfer between slender cylinders and ambient fluids have been studied by two different types. One type is the problem of a steady flow over a stationary slender cylinder [1-7]. Another type is the problem of a slender cylinder moving continuously in a quiescent fluid [8-13]. However, in many engineering systems both the cylinders and the ambient fluids are moving in parallel.

Examples are the cooling of hot fibers issue from a die or slot with a constant surface speed u_s in a parallel free stream u_∞. The problem of a moving surface in a free stream had been analyzed by Adbelhafez [14]. He obtained numerical solutions of the governing boundary layer equations and Navier-Stokes equations. Chappdi and Gunnerson [15] solved the same problem by using an integral technique along with a perturbation procedure. Afzal et al. [16] employed a composite velocity to deal with the problem of a continuous flat plate moving in a parallel stream. Very recently, Lin and Huang [17] studied the general forced convection problem of a surface moving continuously in a flowing stream by using a quite different transformation to obtain similarity solutions. With the exceptions of [4] and [13], in all the studies mentioned above, the fluid considered was Newtonian.

It is well known that a number of industrial fluids exhibit non-Newtonian fluid behavior which may be approximated with the power-law viscosity model. Therefore, in the present paper, the flow and thermal transport from a static or moving cylinder in a quiescent or flowing non-Newtonian fluid are investigated. By introducing novel transformation variables and a parameter of relative velocity, it is able to obtain a set of universal formulation which is readily reducible to the equations of the systems of non-Newtonian fluids flowing over a static slender cylinder and a moving cylinder in a quiescent non-Newtonian fluid. An implicit finite difference scheme is used to solve the reduced system of equations.

Analysis

Consider a steady, laminar, nonsimilar boundary-layer forced convection of non-Newtonian fluids with a free stream velocity u_∞ over a slender cylinder that moves axially with a constant velocity u_s. The physical model and the

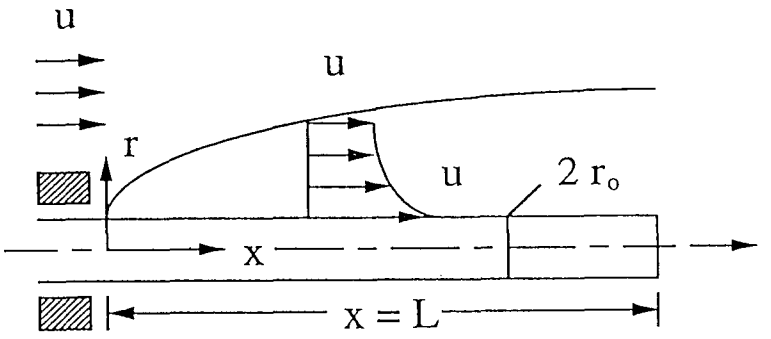

FIG. 1

System schematics and coordinates

coordinate system are depicted in Fig. 1. Neglecting viscous dissipation and wake effects, the governing equations, with the standard power-law viscosity model and constant properties assumption, are

$$\frac{\partial}{\partial x}(ru) + \frac{\partial}{\partial y}(rv) = 0 \tag{1}$$

$$u\frac{\partial u}{\partial x} + v\frac{\partial u}{\partial r} = \frac{K}{\rho r}\frac{\partial}{\partial r}\left[r\left|\frac{\partial u}{\partial r}\right|^{n-1}\left|\frac{\partial u}{\partial r}\right|\right] \tag{2}$$

$$u\frac{\partial T}{\partial x} + v\frac{\partial T}{\partial r} = \frac{\alpha}{r}\frac{\partial}{\partial r}\left(r\frac{\partial T}{\partial r}\right) \tag{3}$$

The associated boundary conditions are

$$\text{at } r = r_o\text{: } u = u_s,\ v = 0 \text{ and } T = T_s \tag{4a}$$

$$\text{as } r \to \infty \text{ : } u = u_\infty \text{ and } T = T_\infty \tag{4b}$$

In order to facilitate the numerical solution, the x-dependence of certain terms in the governing equations is reduced and the boundary conditions are simplified. This is accomplished with coordinate transformations based on a proper choice of transformation parameter derived from scale analysis (cf. ref[18])

$$\xi = \frac{x}{L} \tag{5}$$

$$\eta = \frac{r^2 - r_o^2}{2\, r_o\, L}(\mathrm{Re}/\xi)^{1/(n+1)} \tag{6}$$

$$\Psi = r_o \alpha (Re\ \xi)^{1/(n+1)} F(\xi,\eta) \tag{7}$$

$$\theta = \frac{T - T_\infty}{T_s - T_\infty} \tag{8}$$

where Re is the generalized Reynolds number defined as

$$Re = \frac{\rho U^{2-n} L^n}{K} \tag{9}$$

with L being the length of the cylinder and $U = u_s + u_\infty$ being a composite velocity.

Using the stream function approach

$$u = \frac{1}{r}\frac{\partial \Psi}{\partial r} \text{ and } v = -\frac{1}{r}\frac{\partial \Psi}{\partial x} \tag{10a,b}$$

the continuity equation is automatically satisfied and the momentum and energy equations are transformed to

$$Pr^{2-n}[(1+\epsilon\eta\xi^{1/(n+1)})^{(n+1)/2}|F''|^{n-1}F'']' + \frac{1}{n+1} F F'' = \xi\left[F'\frac{\partial F'}{\partial \xi} - F''\frac{\partial F}{\partial \xi}\right] \tag{11}$$

and

$$\xi^{(n-1)/(n+1)}[(1 + \epsilon\eta\xi^{1/(n+1)})\theta']' + \frac{1}{n+1} F \theta' = \xi\left[F'\frac{\partial \theta}{\partial \xi} - \theta'\frac{\partial F}{\partial \xi}\right] \tag{12}$$

where ϵ is the transverse curvature parameter

$$\epsilon = \frac{2}{r_o}\frac{L}{Re^{1/(n+1)}} \tag{13}$$

Pr is the generalized Prandtl number

$$Pr = \frac{U L}{\alpha} Re^{-2/(n+1)} \tag{14}$$

The corresponding boundary conditions are

$$F(\xi,0) = 0,\ F'(\xi,0) = \gamma\ Pr \text{ and } \theta(\xi,0) = 1 \tag{15a}$$

$$F'(\xi,\infty) = (1-\gamma)\ Pr \text{ and } \theta(\xi,\infty) = 0 \tag{15b}$$

The primes denote partial differentiation with respect to η and γ is the relative velocity parameter defined as

$$\gamma = \frac{u_s}{u_\infty + u_s} \tag{16}$$

Noted that for the case of a steady flow over a stationary cylinder, $u_s = 0$, therefore $\gamma = 0$. On the other hand, for the case of a moving cylinder in a

quiescent ambient fluid, $u_\infty = 0$, and thus $\gamma = 1$.

With the definition of local Nusselt number

$$Nu = \frac{h\,x}{k} \tag{17}$$

a dimensionless local heat transfer group can be formed as

$$HTG = Nu/Re_x^{1/(n+1)} = -\theta'(\xi,0) \tag{18}$$

where

$$Re_x = \frac{\rho\, U^{2-n}\, x^n}{K} \tag{19}$$

is the generalized Reynolds number based on x.

Numerical Solution

The system of transformed equations with the associated boundary conditions were solved by an implicit finite difference technique. This technique is a modified version of that described in [19]. The convergence criterion used was $|(\omega_{ij}^{k+1} - \omega_{ij}^{k})/\omega_{ij}^{k+1}|_{max} < 10^{-4}$ where ω^k and ω^{k+1} are the values of the kth and (k+1)th iteration of F, F', F'', θ or θ'.

The two-dimensional mesh is nonuniform in order to accommodate both the steep velocity and temperature gradients at the wall, particularly in the vicinity of the leading edge of the cylinder. The largest nonuniform mesh consisted of 83 nodal points in the ξ-direction and 289 nodal points in the η-direction. The ratio of lengths of any two adjacent intervals is a constant; this is, $\eta_j = \eta_{j-1} + h_j$, where $h_j = K\, h_{j-1}$. There are two parameters: h_1, the length of the first $\Delta\eta$ step, and K, the ratio of two successive steps. In present study, it takes $h_1 = 0.001$ and $K = 1.02$. The location of the boundary edge, η_e, is strongly dependent on the Prandtl number and the power-law viscosity index. For example, η_e (Pr = 10, n = 1.5) = 6 but η_e (Pr = 100, n = 0.5) = 15.

Numerical error testing has been accomplished by straight-forward repeat calculations with finer meshes to check grid-independence of the results and by local mesh refinement with smooth transitions to coarser regions.

Results and Discussion

In order to verify the accuracy of the present computer simulation model, the results for special case studies are compared with data sets published in the open literature. Table 1 lists the data comparison for the case of Newtonian fluids flow over stationary cylinders. Table 2 contains local heat transfer group comparison for the case of a cylinder that is moving with a uniform velocity in a quiescent Newtonian fluid. In table 3, the values of $Nu/Re_x^{1/(n+1)}$ are compared with the data given by Huang and Chen [20] for forced convection of different Newtonian fluids over a flat plate.

The dimensionless function, $F'(\xi,\eta)$, is related to the streamwise velocity $u(x,y)$ via the transformation given in the previous section as follows.

$$u = (\alpha/L)\, Re^{2/(n+1)}\, F'(\xi,\eta) \tag{20}$$

The step-by-step variations of the profiles of the dimensionless velocity $F'(\xi,\eta)$ from the limiting case of convective heat transfer from a static cylinder in a non-Newtonian fluid free stream ($\gamma = 0$) to the other limiting case of a moving cylinder in a quiescent non-Newtonian fluid ($\gamma = 1$) is shown in Figure 2(a) and 2(b) for pseudoplastics and dilatant fluids, respectively. For the special case of $u_s = u_\infty$ ($\gamma = 0.5$), the velocity profiles are uniform as can be seen from Figs. 2(a) and 2(b). In addition, it is noted that the momentum boundary-layer thickness decreases measurably with increasing power-law viscosity index n. Representative dimensionless temperature profiles within the thermal boundary layer at $\xi = 1$ are demonstrated in Figs. 3(a) and

Table 1.

Data comparison for convective heat transfer along a stationary cylinder in flowing Newtonian fluids; Pr = 0.7, n = 1, γ = 0

	$\frac{d^2f}{d\eta^{*2}}\Big\|_{\eta^*=0}$		$-\frac{d\theta}{d\eta^*}\Big\|_{\eta^*=0}$	
ξ^*	Chen & Mucoglu (1975)	Present method	Chen & Mucoglu (1975)	Present method
0	1.3282	1.3281	0.5854	0.5853
1	1.9172	1.9178	0.8669	0.8674
2	2.3981	2.3999	1.0968	1.1003
3	2.8270	2.8352	1.3021	1.3147
4	3.2235	3.2458	1.4921	1.5211

$$\xi^* = \frac{4}{r_o}(\nu x/u_\infty)^{1/2} \; ; \; f = \frac{\Psi}{r_o(\nu u_\infty x)^{1/2}}; \; \eta^* = \frac{r^2 - r_o^2}{4\, r_o}\left(\frac{u_\infty}{\nu\, x}\right)^{1/2}$$

Table 2.

Data comparison of $Nu/Re_x^{1/(n+1)}$ for a moving cylinder in a quiescent Newtonian fluid; Pr = 10, n = 1, γ = 1

ξ^{**}	Karnis & Pechoc (1978)	Pop et al. (1990)	Present method
0.0001	1.68432	1.68022	1.68394
0.0005	1.68929	1.68026	1.68882
0.001	1.69301	1.68031	1.69250
0.005	1.70870	1.68071	1.70783
0.01	1.72042	1.68121	1.71932
0.04	1.76025	1.68419	1.75783
0.05	1.76960	1.68518	1.75783
0.06	1.77805	1.68617	1.77490
0.07	1.78581	1.68716	1.78231
0.1	1.80617	1.69013	1.80167
0.5	1.95768	1.72926	1.94300
1.0	2.06826	1.77712	2.04348
1.4	2.13615	1.81462	2.10436

$$\xi^{**} = \frac{\nu\, x}{u_s\, r_o^2}$$

Table 3.

Data comparison of $Nu/Re_x^{1/(n+1)}$ for non-Newtonian fluids flow over a flat plate; Pr = 10, ϵ = 0, γ = 0

n	ξ	Huang & Chen (1984)	Present method
0.5	0.01	0.4170	0.41463
	0.1	0.5426	0.53839
	1.0	0.7034	0.69899
1.5	0.01	1.0544	1.04576
	0.1	0.8967	0.89657
	1.0	0.7683	0.76849

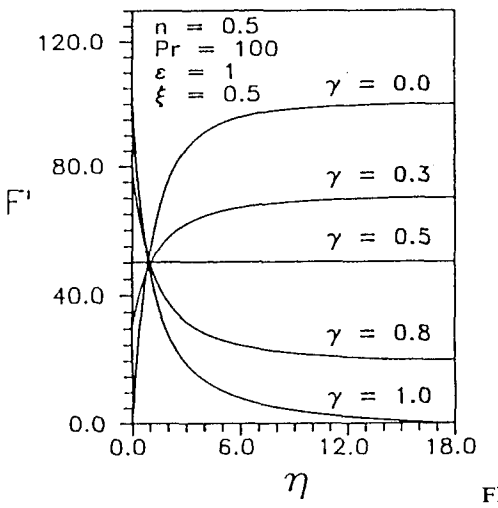

2(a)

Variations of $F'(\xi,\eta)$ with respect to relative velocity parameter γ at ξ = 1 for pseudoplastics

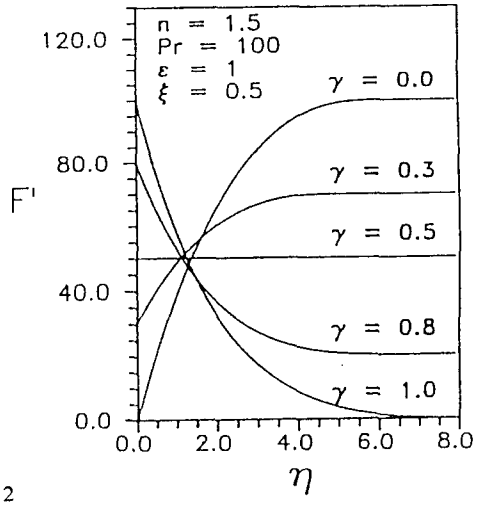

FIG. 2

2(b)

Variations of $F'(\xi,\eta)$ with respect to relative velocity parameter γ at ξ = 1 for dilatant fluids

3(b) for two different types of fluids. It is evident that the dimensionless temperature gradient at the surface decreases monotonously with decreasing values of γ. Another general observation is that the profiles of $\theta(\xi,\eta)$ for pseudoplastics and dilatant fluids are very similar.

The variations of local heat transfer group (HTG) with the representative velocity parameter for specified transverse curvature ($\epsilon = 1$) are depicted in Figs. 4(a) and 4(b) for power-law indices n = 0.5 and n = 1.5, respectively. It is seen that HTG increases as γ increases for both cases of pseudoplastics and dilatant fluids. The significantly behavior of local heat transfer group near $\xi = 0$ for the two non-Newtonian fluids can be explained as given in Wang and Kleinstreuer [4]. Therefore, for $\xi \to 0$, the coefficient of the highest derivative in the energy equation (12) is dominant for pseudoplastics and very small for dilatant fluids. Specially,

$$\xi^{(n-1)/(n+1)} \begin{cases} \to \infty \text{ for } n < 1 \\ \to 0 \text{ for } n > 1 \end{cases} \tag{21}$$

which implies that different values for the local heat transfer group are generated.

The effects of power-law viscosity index and the generalized Prandtl number on the local heat transfer group are shown in Figs. 5(a) and 5(b) for $\gamma = 0$ and $\gamma = 1$, respectively. As expected, the local heat transfer group attains larger values with higher generalized Prandtl numbers. The case of a moving cylinder in a quiescent fluid ($\gamma = 1$) generates larger HTG values than the case of a stationary cylinder in a free stream ($\gamma = 0$) for all types of fluids. Moreover, for the case of $\gamma = 0$, the magnitude of HTG near the leading edge is higher for dilatant fluids and low for pseudoplastics. As ξ increases, the difference reduces quickly and at certain ξ-values, for a given generalized Prandtl number, the HTG numbers for pseudoplastics exceed those of

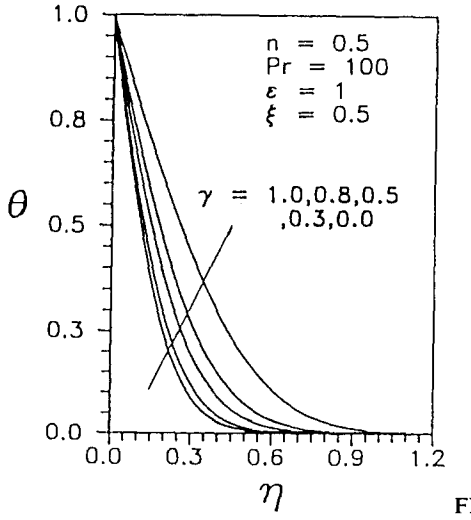

3(a)

Variations of $\theta'(\xi,\eta)$ with respect to relative velocity parameter γ at $\xi = 1$ for pseudoplastics

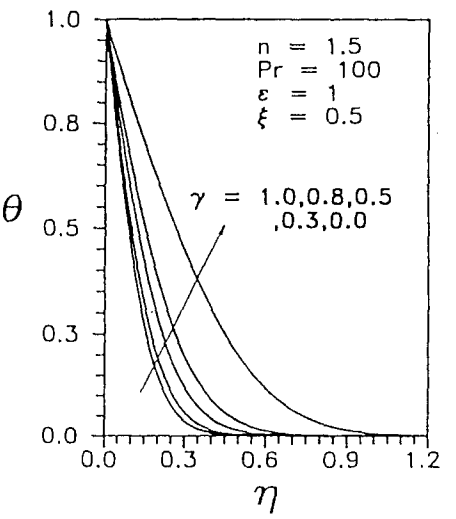

3(b)

FIG. 3

Variations of $\theta'(\xi,\eta)$ with respect to relative velocity parameter γ at $\xi = 1$ for dilatant fluids

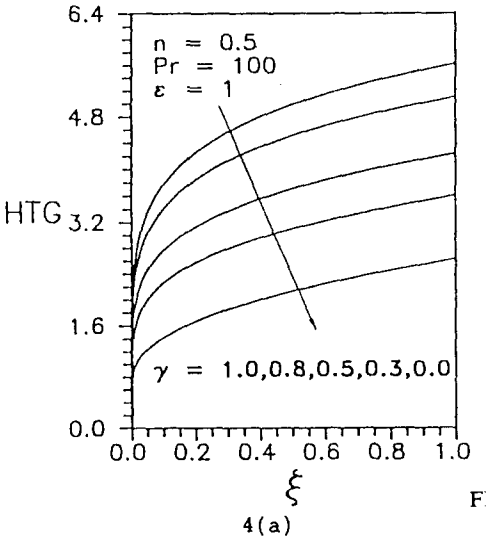

4(a)

The influence of relative velocity parameter HTG distribution for pseudoplastics

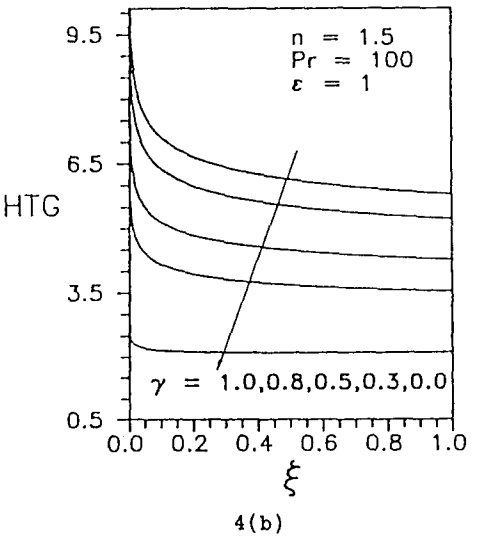

4(b)

FIG. 4

The influence of relative velocity parameter HTG distribution for dilatant fluids

dilatant fluids. On the other hand, for the case of $\gamma = 1$, the values of HTG for both non-Newtonian fluids seem to approach asymptotically the constant HTG values for the equivalent Newtonian fluid.

To illustrate how the transverse curvature and relative velocity affect the heat transfer group, representative HTG distributions are given in Fig. 6. It is found that an increases in either transverse parameter or relative velocity parameter leads to an increases in HTG. Furthermore, the influence of transverse curvature parameter on HTG is more pronounced at high relative velocity parameter.

Conclusions

A generalized analysis of laminar convective heat transfer between a slender cylinder and non-Newtonian fluids has been presented. By introducing a

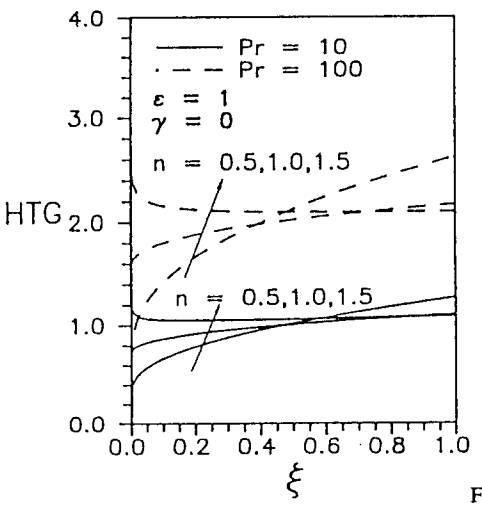

5(a)

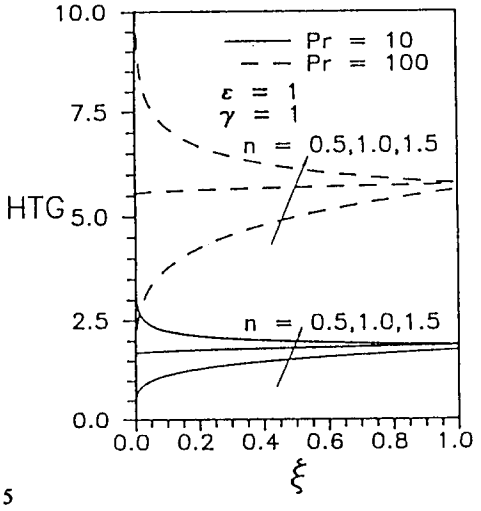

5(b)

FIG. 5

The effects of power-law viscosity index and generalized Prandtl number on HTG distribution for fluids flowing past a static cylinder

The effects of power-law viscosity index and generalized Prandtl number on HTG distribution for a cylinder moving through a quiescent fluid

proper relative velocity parameter together with appropriate coordinate transformations, it is able to obtain a set of universal formulation which is valid over the entire forced convection heat transfer of various values of relative velocity parameters from a non-Newtonian fluid flow over a static slender cylinder to a moving cylinder in a quiescent non-Newtonian fluid. Of particular interest are the effects of the relative velocity parameter, the power-law viscosity index, the transverse curvature parameter and the generalized Prandtl number on the local heat transfer rates as well as on the velocity and temperature profiles.

The distribution of local heat transfer group for non-Newtonian fluids near the leading edge is distinctly different from those of Newtonian fluids. While the momentum boundary-layer thickness increases measurably with decreasing power-law viscosity index n, the thermal boundary-layer thickness

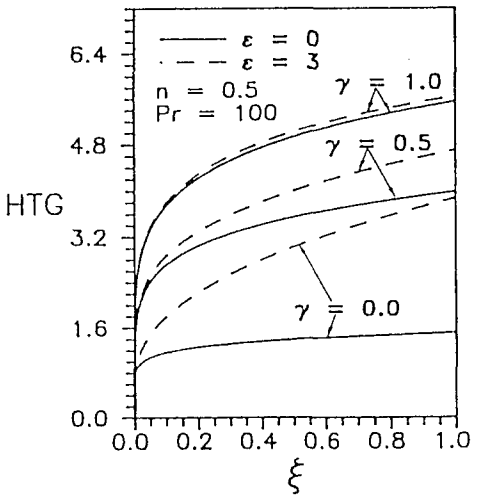

FIG. 6

The effects of transverse curvature parameter and relative velocity parameter on HTG distribution for pseudoplastics

is less affected by the changes in n. An increase in ϵ, γ or Pr increases the HTG values for all types of fluids. Moreover, the influence of transverse curvature parameter on HTG is more profound for high relative velocity parameters.

Acknowledgements

The support of the National Science Council, R.O.C. (Grant No. NSC 83-0117-c-131-016E) for this work is gratefully acknowledged.

References

1 M. N. Bui and T. Cebeci, ASME J. Heat Transfer, 107, 476 (1985).

2. T. S. Chen and A. Mucoglu, ASME J. Heat Transfer, 97, 198 (1975).

3. S. L. Lee, T. S. Chen and B. F. Armaly, Proceedings of The Eighth International Heat Transfer Conference, 3, 1425 (1986).

4. T. Y. Wang and C. Kleinstreuer, Int. J. Heat Mass Transfer, 31, 91 (1988).

5. J. J. Heckel, T. S. Chen and B. F. Armaly, Int. J. Heat mass Transfer, 32, 1431 (1989).

6. T. Y. Wang and C. Kleinstreuer, ASME J. Heat Transfer, 111, 393 (1989).

7. H. Khouaja, T. S. Chen and B. F. Armaly, Int. J. Heat Mass Transfer, 34, 315 (1991).

8. B. C. Sakiadis, AIChE J. 7, 467 (1969).

9. J. W. Rotte and J. W. Beek, Chem. Engng Sci., 24, 705 (1969).

10. D. E. Bourne and D. G. Elliston, Int. J. Heat Mass Transfer, 13, 583 (1970).

11. J. Vlegaar, Chem. Engng Sci., 32, 1517 (1977).

12. J. Karnis and V. Pechoc, Int. J. Heat Mass Transfer, 21, 43 (1978).

13. I. Pop, M. Kumari and G. Nath, Int. J. Engng Sci., 28, 303 (1990).

14. T. A. Abdelhafez, Int. J. Heat Mass Transfer, 28, 1234 (1985).

15. P. R. Chappidi and F. S. Gunnerson, Int. J. Heat Mass Transfer, 32, 1383 (1989).

16. N. Afzal, A. Badaruddin and A. A. Elgarvi, Int. J. Heat Mass Transfer, 36, 3399 (1993).

17. H. T. Lin and S. F. Huang, Int. J. Heat Mass Transfer, 37, 333 (1994).

18. A. Bejan, *Convection Heat Transfer*, Chap. 4, Wiley, New York (1984).

19. B. Carnahan, H. A. Luther and J. O. Wikes, *Applied Numerical Methods*, Chap. 7, Wiley, New York (1969).

20. H. J. Huang and C. K. Chen, Int. Comm. Heat Mass Transfer, 11, 361 (1984).

Received June 20, 1995